ELSEVIER

Journal of Molecular Catalysis A: Chemical 189 (2002) 271–282

JOURNAL OF MOLECULAR CATALYSIS A: CHEMICAL

www.elsevier.com/locate/molcata

Preparation, physico-chemical characterization and catalytic activity of sulphated ZrO_2–TiO_2 mixed oxides

D. Das [a], H.K. Mishra [a], K.M. Parida [b], A.K. Dalai [a,*]

[a] *Catalysis and Chemical Reaction Engineering Laboratories, Department of Chemical Engineering, University of Saskatchewan, 110 Science Place, Saskatoon, Canada, S7N 5C9*

[b] *Environment Management and Inorganic Chemicals Division, Regional Research Laboratory, Bhubaneswar, Orissa 751 013, India*

Received 22 February 2002; received in revised form 2 July 2002; accepted 2 July 2002

Abstract

A series of ZrO_2–TiO_2 mixed oxides was prepared varying mole fraction of titanium from 0 to 1, and characterized by XRD, FT-IR, TG/DTA, UV–VIS–DRS, surface area, surface acidity, and sulphur content. The UV–VIS–DRS and pH of point of zero charge (pH_{ZPC}) data for the mixed oxide samples determined by acid–base titration method revealed that a different surface was formed when zirconium and titanium were co-precipitated. XRD pattern of 700 °C calcined samples showed the formation of $ZrTiO_4$ phase. The optimum concentration of zirconium in the zirconia–titania mixed oxide in the precipitation solution was 60 mol% for obtaining high surface area and highly acidic mixed oxide system. Sulphur analysis of the sulphate promoted samples showed that the sample containing Ti mole fraction 0.4 retained the highest amount of sulphur. The surface acidity determined by irreversible adsorption of organic bases, such as pyridine, piperidine and 2,6-dimethyl pyridine showed the highest acidity for the above sample. This catalyst also showed the highest catalytic activity towards isopropanol dehydration.

Keywords: ZrO_2–TiO_2 mixed oxide; Structural stability; Surface acidity; 2-Propanol dehydration

1. Introduction

The fast deterioration of environment has sought the replacement of environmentally hazardous liquid acid and base catalysts, such as HF, H_2SO_4, HCl, $Ca(OH)_2$, etc. used by several oil refineries and chemical industries. Other important issues regarding their use are problems related to separation from product stream, significant wastage, cost of process installation and maintenance. The phenomenal breakthrough came with the development of solid acid and base catalysts [1] and is gradually gaining importance in the catalytic field. Solid acid catalysts have the additional advantage that the nature of the active sites are known and may be defined by the presence of surface protons generating Bronsted acidity or coordinately unsaturated cationic centers, i.e. Lewis acid sites [2]. Metal oxides, such as ZrO_2, TiO_2, Fe_2O_3, etc. when modified with sulphate, develop strong acidity, and act as a potential catalyst for low temperature isomerization, esterification, alkylation and cracking reactions [3–6]. Sulphate promoted zirconium oxide became the center of investigation due to its high thermal and mechanical stability, low reducibility [7,8] as well as the lower

* Corresponding author. Tel.: +1-306-966-4771; fax: +1-306-966-4777.
E-mail address: dalai@engr.usask.ca (A.K. Dalai).

1381-1169/02/$ – see front matter © 2002 Elsevier Science B.V. All rights reserved.
PII: S1381-1169(02)00363-1

reactivity with respect to the active phases. However, the disadvantages of sulphated zirconia are that the active sites are limited due to availability of specific surface area [9] and fast deactivation due to coke formation and sintering [10]. Similar problems are also encountered for sulphated titania, which have been studied for several reactions, such as isomerization, alkylation and esterification [2]. Furthermore, its active anatase phase has poor stability at high temperature. Therefore, much attention has been focussed on the development of mixed oxide catalysts [11,12]. It has also been observed that the thermal resistance of zirconia can be enhanced considerably by the incorporation of a second metal oxide [13,14]. It is also possible to develop a much more active and selective catalyst by the incorporation of a transition metal, especially noble metals, into the zirconia framework [15,16]. The mixed oxides often show enhanced acidity in comparison to the respective single component oxides. The most widely accepted model for the generation of acid sites on the mixed oxides is that the surface acidity results from the charge imbalance [17]. Though this model explains almost 90% predictions about mixed oxide acidity [18,19], it fails to explain the highest acidity for 50–50 mol% mixed oxide system [20]. But the recent modifications still rely on the charge imbalance resulting from heteroatom linkages for the creation of acid centers [21].

The properties of catalysts are strongly dependent on the preparation methods including the precipitation conditions, nature of precursors used, thermal treatment, etc. [1,2,22]. It has been observed that the surface area of ZrO_2–TiO_2 mixed oxide changes parallel to the TiO_2 content and passes through a maximum at about equimolar ratios [18]. In view of the importance of ZrO_2 in several industrially important reactions and to modify the physical and textural properties, such as surface area, thermal stability, surface acidity, etc. a series of ZrO_2–TiO_2 mixed oxide was prepared by co-precipitation method varying Ti mole fractions. The previous report [18] showed that the 50:50 Zr:Ti molar ratio mixed oxide imparted highest surface area and acidity. In this work, we have investigated the physico-chemical and textural properties, in addition to other molar ratios, for two close variations to 50:50 ratios. Further, the catalytic activity was tested taking isopropanol dehydration as the probe reaction.

2. Experimental

2.1. Material Synthesis

A series of ZrO_2–TiO_2 was prepared by co-precipitation method taking $ZrOCl_2$ and $TiCl_4$ (Merck, India) as the precursor material. The mixture of acetyl acetone, ethyl alcohol and ammonium hydroxide was stirred in a stainless steel reactor for about 10 min and the required amount of premixed $ZrOCl_2$ + $TiCl_4$ solution was added to this under vigorous stirring conditions and kept for another 20 min. This procedure was followed in order to avoid the local precipitation effect. The basic colloidal solution was charged in the reactor for hydrothermal reaction for 6 h at 110 °C (not stirred). The precipitate was filtered, washed with deionized water until it became free of chloride ions (negative $AgNO_3$ test), and dispersed three times in distilled ethanol. The precipitate was then dried initially at 60–70 °C for 5–6 h and then at 110 °C overnight. The dried gels were contacted with 0.25 M H_2SO_4 solution (15 ml/g of sample) stirred for 1 h, filtered (not washed) and dried again at 110 °C overnight. The sulphate-promoted mixed oxides were obtained by calcining the sulphated gels at 600 and 700 °C in static air.

2.2. Characterization

2.2.1. Sulphur content

The sulphur content in 600 °C calcined samples was analyzed nephelometrically in the water extract after Na_2O_2 fusion. Photonephelometry was used for sulphur analysis by employing the procedure reported earlier [23]. Nephelometric method of analysis is based on the principle in which light passed through a medium with dispersed particles of different refractive index than the medium, is attenuated in intensity by scattering.

2.2.2. X-ray diffraction

The crystallographic phase identification studies of the 700 °C calcined samples were performed in an X-ray powder diffractometer (XRD 7, Rich. Seitest and Co., Freiberg) with Cu Kα radiation. The samples were scanned in the range of $2\theta = 10$–70° at a scanning speed of 2°/min.

2.2.3. FT-IR spectroscopic studies

To determine the nature and types of groups and their bonding with ZrO_2–TiO_2 mixed oxides, all 600 °C calcined samples were characterized by FT-IR spectroscopy in KBr phase using FT-IR spectrophotometer (Parkin-Elmer, Paragon-500) attached to an automatic data acquisition center. Prior to measurement, all samples were dried at 110 °C for 24 h.

2.2.4. Surface area analysis

The specific surface area of the samples was determined using N_2 adsorption/desorption method at 77 K by standard BET method (Quantasorb, Quantachrome, USA). Prior to each measurement all samples were degassed at 110 °C and 10^{-4} Torr pressure to evacuate the physisorbed moisture.

2.2.5. pH of zero point charge (pH_{ZPC})

The pH_{zpc} (zero point charge) of the 600 °C calcined ZrO_2–TiO_2 samples was determined by potentiometric acid–base titration by suspending 0.1 g of the sample in 50 ml of 0.1, 0.01 and 0.001 mol/l KNO_3 as supporting electrolyte following the method of Parks and de-Bruyn [24].

2.2.6. Surface acidity

Acidity of all the samples was determined by the irreversible adsorption of organic bases, such as pyridine (PY, $pK_a = 5.1$), piperidine (PP, $pK_a = 11.1$) and 2, 6-dimethylpyridine (DMPY, $pK_a = 6.7$) in liquid phase. The measurement procedure has been reported elsewhere [25].

2.2.7. Thermal studies

The TG/DTA analysis of the 110 °C dried samples was carried out in a Shimadzu DT-40 Thermal Analyzer in the range of 30–1000 °C in N_2 atmosphere. The heating rate was maintained at 10 °C/min.

2.2.8. UV–VIS–DRS spectroscopy

The UV–VIS spectra of the 600 °C calcined samples were recorded in a Varian UV–VIS–DRS spectrophotometer fitted with Carry 100 software. The spectra were recorded against the boric acid background.

2.3. Catalytic activity

The catalytic activity of sulphated zirconia–titania mixed oxides calcined at 600 °C, was studied for dehydration of isopropanol in a fixed bed reactor (10 mm i.d. and 45 cm long) connected to an online GC (CIC, India). Prior to reaction, all catalysts were pretreated at 400 °C for 2 h in N_2 atmosphere. Isopropanol was supplied to the reactor from a continuous micro feeder (Orion, USA) through a vaporizer using N_2 as the carrier gas (flow rate 60 ml/min). All the connections from the feeder to the GC were heated at about 80 °C by a heater coil in order to avoid product condensation. The products were analysed by the GC in FID mode using a Porapack Q packed column.

The rates of alcohol conversion were calculated under steady state conditions by applying the equation:

$$X = r\left(\frac{W}{F}\right)$$

where r is the rate of reaction, W the weight of the catalyst, F the flow rate of the reactant, and X the percentage of conversion.

The rates were calculated from the slopes of the straight lines obtained by plotting X against F^{-1}. The kinetic parameters were calculated for dehydration of isopropanol to propene. The conversion of isopropanol to propene was limited within 20 mol% in order to keep the reaction in the kinetic regime.

3. Results and discussion

3.1. Crystalline phases

The detailed study of the crystalline phases is necessary as their nature can greatly influence the catalytic behavior of the materials. For example, the anatase to rutile phase transformation is considered to play a major role in catalyst deactivation in selective oxidation catalysts [26]. Since Zr and Ti belong to the same group (IV B), they are expected to have similar properties and when they are co-precipitated the chemical interaction might be profound. In fact, it has been seen in this case that addition of titania as a second oxide-component hinders the crystallization of pure zirconia. Similar observation was also reported earlier [18].

All the 110 °C dried samples were found to be XRD amorphous, and so also 600 °C calcined samples if neither the Zr nor the Ti content is less than 20 mol% (patterns not given). A similar observation was made

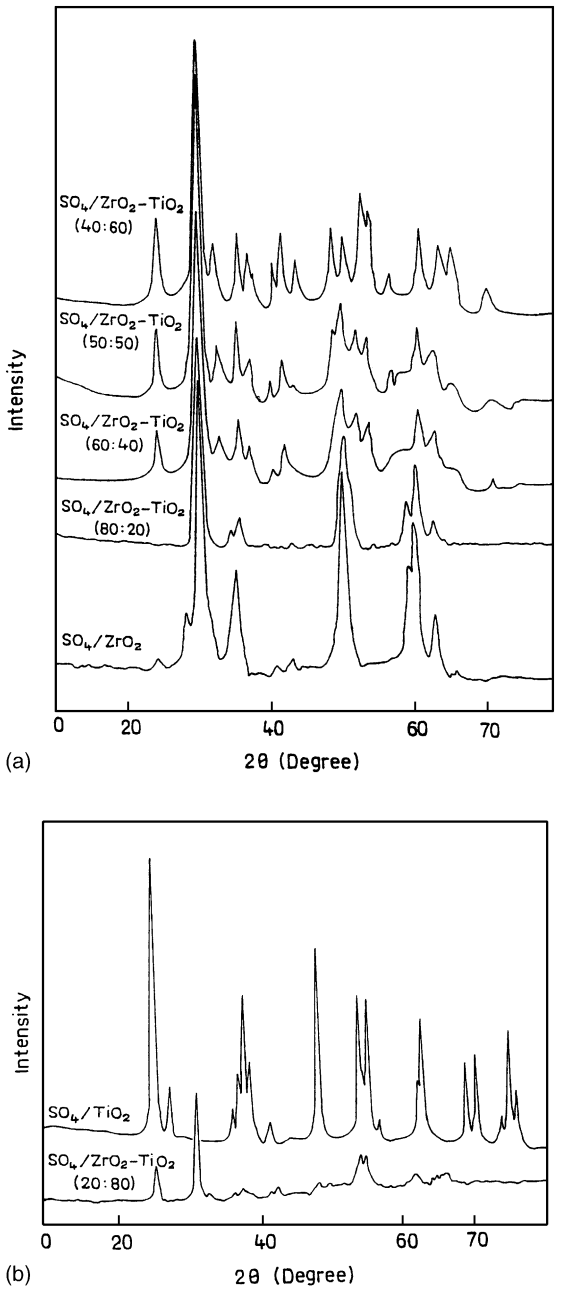

Fig. 1. (a) and (b): XRD pattern of ZrO_2–TiO_2 mixed oxides prepared at different Ti mole fractions and calcined at 700 °C.

by Wang et al. [27]. Fig. 1a and b shows the XRD pattern of the sulphated samples calcined at 700 °C. It is seen that sulphated zirconia and sulphated titania contained tetragonal and anatase phases, respectively. However, addition of titanium to zirconia resulted in $ZrTiO_4$ phase. It may be noted here that $ZrTiO_4$ phase (cf. Fig. 1, peak at $2\theta \sim 30^\circ$) is difficult to distinguish from tetragonal zirconia. But, the intensity of 202 peak of zirconia (at $2\theta \sim 52^\circ$) suggests that the peak at $2\theta \sim 30^\circ$ in the case of samples containing titanium is due to $ZrTiO_4$ phase [28]. Lonyi and Valyon [28] have found the anatase phase in sulphated titania below 550 °C, and according to them, anatase to rutile phase transfer occurs with a rise in temperature above 550 and 650 °C calcined samples contained rutile phase in considerable amount. But we found anatase titania even at a calcination temperature of 700 °C. On the other hand, as discussed above, the mixed oxides containing 0.4, 0.5 and 0.6 mole fractions of Ti showed diffraction pattern only for $ZrTiO_4$ phase in XRD spectra (Fig. 1a). None of them has developed either of the single phases, which indicate that these materials are the mixed oxides of zirconium and titanium. For mixed oxide containing 50 mol% Ti, the fact is well understood. But, when, the concentration of one component is higher than the other one, it is generally expected to get an additional XRD peak for single (major component) metal oxide. But this was not observed in our case. This could be due to the presence of major single component oxide in more dispersed state over the mixed oxide surface forming very small crystallites, which were not large enough to be detected by XRD. A similar observation was made by Linacero et al. for Al_2O_3–TiO_2 mixed oxides [29]. When either Zr or Ti content is 20 mol%, a poorly developed diffraction pattern was seen for the major component oxide (e.g. in Fig. 1a, graph 2, the 35% peak for tetragonal ZrO_2 at $2\theta = 52^\circ$ is still present, but the peak intensity is less. This peak intensity further diminished and it splited into several peaks, which differentiated $ZrTiO_4$ from tetragonal ZrO_2). This poorly developed X-ray diffraction peaks for major component oxide in the case of sample containing 20 mol% Zr or Ti may be due to formation of slightly larger crystals than the samples containing higher amounts of Zr and Ti.

3.2. Zero point charge (ZPC)

The zero point charge (ZPC) of the catalyst indicates that for pH values above pH_{ZPC}, the surface becomes negatively charged, and conversely that below the ZPC value it becomes positively charged.

Its importance is mostly felt during the impregnation step of the active phase, preferably in aqueous solution where the active metals are present either as cations or anions. The technique of electrophoretic migration of ions has been adopted as a popular tool to determine the ZPC of catalyst supports [24,30]. Table 1 represents a summary of the ZPC values of the series, where one can easily observe that with progressive increase of TiO_2 content in the mixed oxide, the pH_{ZPC} value decreases and again increases after passing through a minimum at equimolar compositions. Dominguez et al. [31] followed the mass titration method to find out the ZPC of Al_2O_3–ZrO_2 mixed oxides. They observed that the pH_{ZPC} values of alumina–zirconia mixed oxides are lower than that of the single oxide. Based on this observation, they argued in favor of the formation of a new phase at the surface level, i.e. Al_2O_3–ZrO_2 solid solution. In the present case, the pH_{ZPC} values of the zirconia–titania mixed oxide system are always less than that for the pure oxides. This observation supports that a different phase has formed at the surface when zirconia and titania are co-precipitated. This conclusion is also supported by the above described XRD results, that addition of titania to zirconia results in the formation of $ZrTiO_4$.

3.3. Sulphur analysis

Table 1 represents the sulphur content of various samples in the series. The highest sulphur content appears at mixed oxide with titanium mole fraction of 0.4. It seems that the addition of Ti to the system may help in stabilizing the surface sulphate species remarkably. In an earlier study, Xia et al. [32] reported that impregnation of aluminium on zirconia stabilizes sulphate. They argued that framework substitution of aluminium in a zirconia matrix increased the electropositive character of Zr^{4+} resulting in the formation of Zr–O–Al bonds and stabilized the surface sulphate complex. From the XRD and pH_{ZPC} (cf. Table 1 and Fig. 1) analyses results, and above analysis, it appears that the surface of the mixed oxide has Zr–O–Ti bonds. On the other hand, titanium is more electronegative than zirconium. Therefore, formation of solid solution of zirconium and titanium (i.e. Zr–O–Ti) might have increased the electropositive character of zirconium thereby stabilizing sulphate. From Table 1 it is also seen that the sample containing 60 mol% of zirconium has the highest sulphate content. This observation perhaps indicates the surface of the mixed oxide contains maximum amount of the Zr–O–Ti structure, and that a solution containing 60 mol% Zr in a zirconia–titania mixed oxide system is the optimum composition of a solution to develop high degree zirconia–titania solid solution or a mixed oxide system by co-precipitation method.

Table 1
pH_{zpc} and sulphur content of ZrO_2–TiO_2 mixed oxides prepared at different molar ratios and calcined at 600 °C

Sample code	pH_{zpc}	Sulphur content[a] (wt.%)
ZrO_2–TiO_2 (0)	6.8	2.3
ZrO_2–TiO_2 (0.2)	6.2	2.8
ZrO_2–TiO_2 (0.4)	6.05	3.0
ZrO_2–TiO_2 (0.5)	5.96	2.4
ZrO_2–TiO_2 (0.6)	6.06	2.0
ZrO_2–TiO_2 (0.8)	6.45	1.3
ZrO_2–TiO_2 (1.0)	7.04	0.3

Values in parentheses represent Ti mole fractions.
[a] Sulphur contents are measured in the 600 °C calcined sulphated zirconia–titania samples.

3.4. FT-IR study

The background subtracted FT-IR spectra of 110 °C dried sulphated samples have been presented in Fig. 2. The broad peak at 3400 cm^{-1} is attributed to O–H stretching vibration of water associated with the oxide matrix. The peaks at 1205, 1132, 1056 and 1000 cm^{-1} are present in all samples except for 100% TiO_2 sample. All samples show distinct peaks in the region 950–1400 cm^{-1}, characteristic of bidentate sulphate [33]. A strong peak is observed at 1386 cm^{-1} in all samples and it is assigned to $\nu_{S=O}$ stretching vibration of surface sulphate groups. The $\nu_{S=O}$ vibration in free sulphate ion appears at around 1400 cm^{-1} [7]. However, a decrease in the frequency of $\nu_{S=O}$ vibration from 1400 to 1386 cm^{-1} indicates that the strength of the S=O bond has reduced significantly suggesting that sulphate in these samples is strongly covalent in character [7,34]. This band also remains almost undisturbed (no shift) for the whole range of molar ratios of titanium. The strong band observed at 1620 cm^{-1} is characteristic of bending vibration mode of O–H of water associated with the sulphate group [34].

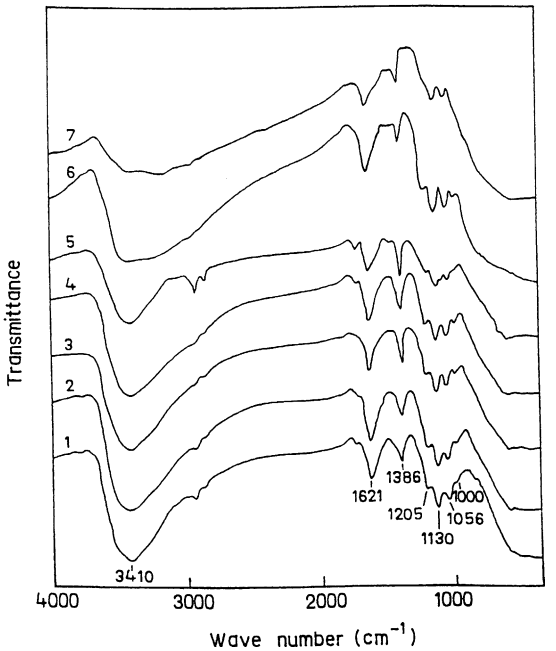

Fig. 2. FT-IR spectra of 110 °C dried sulphated ZrO_2–TiO_2 mixed oxides prepared at different titanium mole fractions. Spectra 1–7 represent for Ti mole fractions 0, 0.2, 0.4, 0.5, 0.6, 0.8 and 1.0, respectively.

From Table 2 it is seen that sulphation of the zirconia–titania mixed oxide enhanced surface area. Aiken et al. [35] reported that sulphate, coordinated to two different atoms (sulphate in bridged form), caused an increase in surface area. The IR patterns

Table 2
Specific surface areas (m^2/g) of ZrO_2–TiO_2 mixed oxides calcined at different temperatures

Sample code	Calcination temperature	
	110 °C	600 °C
SO_4/ZrO_2–TiO_2 (0)	358 (321)	156 (46)
SO_4/ZrO_2–TiO_2 (0.2)	407 (358)	160 (93)
SO_4/ZrO_2–TiO_2 (0.4)	481 (329)	177 (155)
SO_4/ZrO_2–TiO_2 (0.5)	453 (304)	147 (148)
SO_4/ZrO_2–TiO_2 (0.6)	457 (331)	150 (143)
SO_4/ZrO_2–TiO_2 (0.8)	457 (457)	103 (105)
SO_4/ZrO_2–TiO_2 (1.0)	214 (252)	38 (29)

Values in parentheses (column 1) represent the Ti mole fractions; values in parentheses in columns 2 and 3 represent the surface area of corresponding non-sulphated samples.

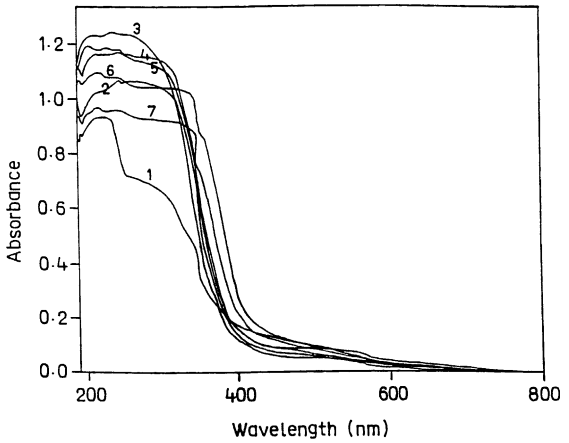

Fig. 3. UV–VIS–DRS spectra of 600 °C calcined sulphated ZrO_2–TiO_2 mixed oxides prepared at different mole fractions. Spectra 1–7 represent Ti mole fractions 0, 0.2, 0.4, 0.5, 0.6, 0.8 and 1.0, respectively.

(cf. Fig. 2) along with the surface area data in Table 2, may suggest that sulphates in these oxides are bidentately coordinated with a bridged structure.

3.5. UV–VIS–DRS spectroscopic study

Fig. 3 depicts the background subtracted UV–VIS–DRS spectra of the series of sulphated samples calcined at 600 °C. A strong absorption band is seen at 215 nm in case of ZrO_2 (spectrum 1) characteristic of ligand to metal charge transfer band of an isolated Zr atom in a tetrahedral geometry [36]. For Ti rich samples, i.e. for Ti mole fractions 0.8 and 1.0, a band at 210 nm, characteristic of tetrahedral titanium (spectra 6 and 7) as indicated Schinder et al. [37], becomes more prominent. These bands are absent in samples with Ti mole fractions 0.4, 0.5 and 0.6 (spectra 3, 4 and 5, respectively). So, we can predict that a new matrix, which is different from the previous case, is formed. This is further supported by XRD and pH_{ZPC} analyses results.

3.6. Textural properties

Table 2 represents the surface areas of various zirconia–titania sulphated and non-sulphated samples. The 110 °C dried non-sulphated samples show quite high surface area without any specific trend with

change in titanium concentration. However, on sulphation the surface area of the samples significantly increased compared to their non-sulphated counterparts except for pure sulphated titania. Also, with increase in titanium content up to 40 mol% surface area gradually increased, then decreased, to some extent, and remained constant until 80 mol%. It has been reported that during sulphation of a hydrated oxide or hydroxide, sulphate groups are chemically exchanged with the hydroxyl groups [22], leading to an open structure in the sulphated oxide thus giving high surface area. However, it is not very clear at this moment why the surface area of the titanium-enriched (Ti >50 mol%) mixed oxides remained almost constant.

The surface areas of the calcined (600 °C) samples (both sulphated and non-sulphated) are significantly lower than that of 110 °C dried; perhaps because of structural modification via sintering. However, the 600 °C calcined sulphated samples containing up to 60 mol% of zirconium show significantly higher surface area compared to their non-sulphated counterparts. It was proposed earlier that the presence of sulphate, phosphate or tungstate hinder the sintering process, increase crystallization temperature and stabilize surface area of zirconia and titania [38,39]. Interestingly, the titanium-enriched (Ti >50 mol%) non-sulphated samples calcined at 600 °C show surface area very similar to the corresponding sulphated oxides, which contain significant amount of sulphate (cf. Table 1). This contradicts the earlier report [38] that sulphate stabilizes the surface area of an oxidic system. Based on this observation we propose that sulphate is not always a determining factor for the surface area stabilization, rather precipitation chemistry of the metal oxide preparation sometimes has greater influence over the mere presence of sulphate on the textural and structural characteristics of the oxide.

3.7. Thermal analysis

The complexity in the zirconium–titanium polymeric system makes it difficult to assign a step of the TG curve to the removal of a particular component. Several components, such as physically adsorbed water, physically and chemically bound alcohol and acetylacetone molecules used in the preparation steps, are expected to be present in the mixed oxides (and also in the single oxides). Fig. 4 depicts the TG curves of sulphated ZrO_2–TiO_2 oxides dried at 110 °C. It is clear that the weight loss is continuous in all cases starting at around 50 °C and up to approximately 850 °C. In addition, two sharp weight losses are observed in all cases except the samples having Ti mole fraction of 0.8 or above. The first step weight loss

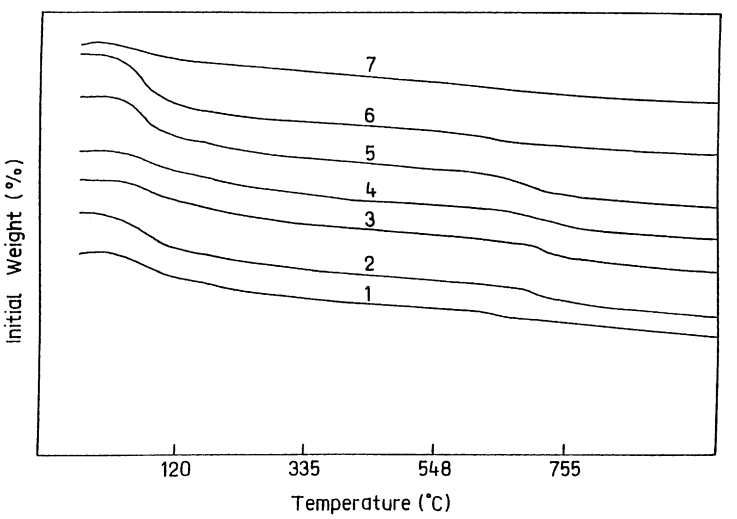

Fig. 4. Thermogravimetric analysis of 110 °C dried sulphated ZrO_2–TiO_2 mixed oxides prepared at different Ti mole fractions. Spectra 1–7 represent Ti mole fractions 0, 0.2, 0.4, 0.5, 0.6, 0.8 and 1.0 respectively.

close to 130 °C may be attributed to the removal of physisorbed water, ethanol, etc. followed by the decomposition of organic groups till 300 °C. The second sharp weight loss at around 700 °C may be due to the sulphate decomposition. The sharpest sulphate loss is seen in the sample with $X = 0.4$ (spectrum 3, Fig. 4).

As discussed earlier, the addition of sulphate or titania to the zirconia system enhances the thermal stability. The changes in crystallization kinetics have been reflected by the shift of the exothermal DTA peak to the higher values (Fig. 5). The exothermic DTA peak arising due to the phase transition is superimposed over the broad endothermal sulphate decomposition [40]. With increase in titania content, the phase transition peak shifts towards higher temperature and then shifts to the lower value after passing through a maximum at about equimolar compositions. The phase transformation temperature for the samples having $X = 0.4$ and 0.5 are the same, i.e. close to 720 °C (spectra 3 and 4 in Fig. 5). But the X-ray diffraction results reveal well-crystallized material, even below this temperature. This may be due to the role of the calcination period, which plays an important role in phase transition [41]. It may be noted here that the samples were treated in nitrogen during DTA and 700 °C calcined (in static air) samples were used for XRD analysis, and therefore a comparison of DTA results with those of XRD may be misleading. In one of the earlier reports, Srinivasan et al. [42] have reported the TG/DTA of sulphated zirconia in helium, and air atmospheres. However, they did not observe any significant difference in the DTA peaks obtained in two different mediums. Based on this report we also believe that the DTA patterns of sulphated zirconia–titania samples in air and in nitrogen would be similar, and therefore, the DTA of the samples obtained in nitrogen can be used to interpret and compare the XRD results. Lonyi and Valyon [28] have reported that for high titania content, the samples having higher surface area go through fast phase transformation. But in this case, high phase-transition temperature is observed for samples with higher surface areas.

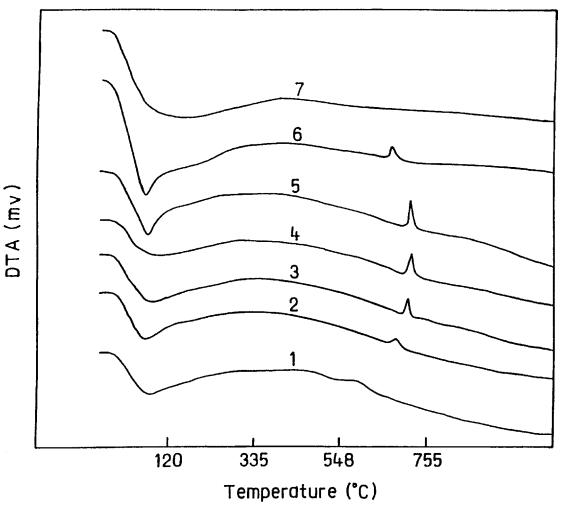

Fig. 5. DTA pattern of 110 °C dried sulphated ZrO_2–TiO_2 mixed oxides prepared at different Ti mole fractions. Spectra 1–7 represent Ti mole fractions 0, 0.2, 0.4, 0.5, 0.6, 0.8 and 1.0, respectively.

3.8. Surface acidity

Mixed oxides often show enhanced acidity in comparison to the respective single component oxides [17,18]. The nature of acid sites may be defined by the presence of surface protons leading to the Bronsted sites or cationic centers arising due to unsaturation in coordination, which explain the Lewis acidity. The acidity is determined by the irreversible adsorption of pyridine (PY) and piperidine (PP) in organic solvent as a function of Ti molar ratios and calcination temperatures. PP being a stronger base adsorbs on all types of acid centers and represents total acidity of the samples. On the other hand, PY adsorbs only on the strong acid sites [25].

Table 3 shows the acidity data of both non-sulphated and sulphated oxide samples. It is seen that both sulphated and non-sulphated materials show increase in acidity with an increase in Ti mole fraction up to 0.4 and thereafter it decreased. Tanabe et al. [17] proposed that acidity of a mixed oxide system is more than that of the pure oxide-components due to the charge imbalance imposed by the major oxide-component upon the minor oxide-component. From the results on XRD, UV–VIS–DRS and pH_{ZPC} analyses (cf. Figs. 1 and 3 and Table 1) we have concluded that the mixed oxide system contains solid solutions of zirconia and titania (Zr–O–Ti), the extent of which is probably maximum with Ti mole fraction 0.4. Therefore, we propose the increase in acidity with the increase in Ti mole fraction up to 0.4 is due to the formation of mixed oxides with an interaction between Zr and Ti atoms through

Table 3
Surface acidity of non-sulphated and sulphated ZrO_2–TiO_2 mixed oxides at different temperatures

Sample code	PY (μmol/g_{cat})		PP (μmol/g_{cat})		DMPY (μmol/g_{cat})
	600 °C[a]	700 °C[a]	600 °C[a]	700 °C[a]	600 °C[a]
ZrO_2–TiO_2 (0)	22	–	76	–	–
ZrO_2–TiO_2 (0.2)	46	–	179	–	–
ZrO_2–TiO_2 (0.4)	104	–	340	–	–
ZrO_2–TiO_2 (0.5)	101	–	338	–	–
ZrO_2–TiO_2 (0.6)	100	–	328	–	–
ZrO_2–TiO_2 (0.8)	80	–	254	–	–
ZrO_2–TiO_2 (1.0)	36	–	68	–	–
SO_4/ZrO_2–TiO_2 (0)	202	67	424	148	99
SO_4/ZrO_2–TiO_2 (0.2)	202	56	435	154	96
SO_4/ZrO_2–TiO_2 (0.4)	226	55	463	186	97
SO_4/ZrO_2–TiO_2 (0.5)	206	38	454	101	85
SO_4/ZrO_2–TiO_2 (0.6)	191	47	394	135	75
SO_4/ZrO_2–TiO_2 (0.8)	149	91	336	117	48
SO_4/ZrO_2–TiO_2 (1.0)	63	35	113	58	19

Values in parentheses represent Ti mole fractions.
[a] Calcination temperature.

oxygen, which also complies with Tanabe's model for the mixed oxide system.

The changing trends in acidity observed for sulphated samples are similar to that of non-sulphated samples; however, with much improved acidity. From FT-IR analysis we know that the sulphate group is bidantately coordinated to the oxide matrix with a bridged structure. This mode of coordination of sulphate may further affect the charge imbalance enhancing the acidity. The PY absorption values for 700 °C calcined samples did not follow any specific trend with changes in Ti content, and the values are also much less, as compared to those obtained in 600 °C calcined samples, indicating that calcination of the samples at 700 °C loses a significant amount of acidity. Similar observations were observed with PP as the probe molecule; however, with higher acidity. After calcinations at 700 °C the material loses sulphate from surface as sulphate decomposition starts beyond 650 °C. This could be the reason for less acidity in case of 700 °C calcined samples. Dimethylpyridine (DMPY) has been used by researchers to quantify the Bronsted acidity in a sample [43]. The number of Bronsted acid sites obtained is much less as compared to those obtained with PP adsorption (cf. Table 3), which indicates that the samples are rich in Lewis acid sites.

4. Catalytic activity

The catalytic activity of the sulphated samples (calcined at 600 °C) was tested for 2-propanol conversion reaction in which propene is found to be the major and diisopropylether (DIPE) as the minor product ($\leq$3 mol%) for the whole series. In addition, formation of acetone is seen ($\leq$1.5 mol%) for titanium rich samples ($X = 0.8$ and 1.0). The absence of acetone formation was obvious as the materials were acidic in nature. But the low acetone formation in titanium rich samples (Ti mole fractions 0.8 and 1.0) may be due to the presence of appropriate amounts of redox sites. Fig. 6 shows the total conversion of 2-propanol (mol%) as a function of reaction temperature, and the comparison was made with respect to per gram of the catalyst weight. Results show that with an increase in reaction temperature, propanol conversion increases. Also, increase in reaction temperature favors propene selectivity because of the reduction in DIPE formation. DIPE is formed by the bimolecular reaction between alcohol and alkene on the active surfaces. So the decrease in DIPE formation, with a rise in temperature, may either be due to reverse reaction i.e. DIPE to propene or inhibition caused by strong adsorption of 2-propanol on active sites. Table 4 shows the rate and other kinetic parameters for the formation

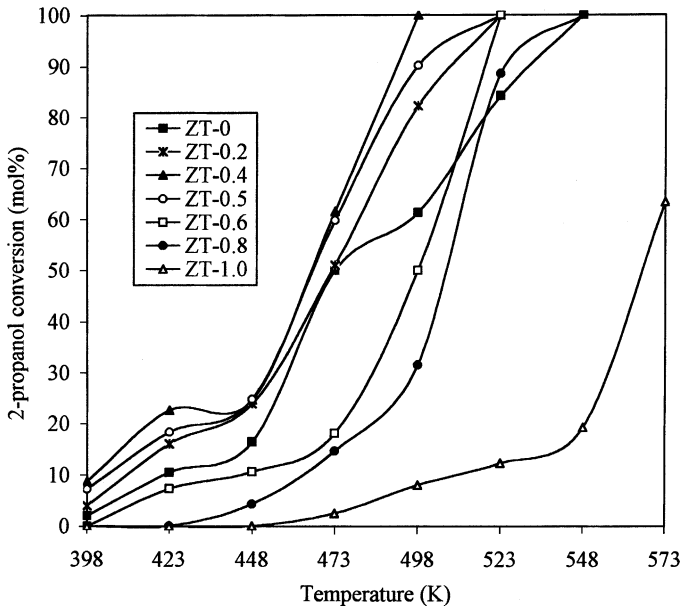

Fig. 6. Percentage of 2-propanol conversion (mol%) as a function of temperature. ZT represents SO_4/ZrO_2–TiO_2 and the fractions represent Ti mole fractions.

of propene from isopropanol. It may be noted here that all kinetic measurements were made under steady state conditions keeping the conversion level of isopropanol to propene (dehydration reaction) below 20%. In all cases, the findings are reproducible within ±5%. For the reaction at 423 K, a wide range of rates was seen with change in titanium content of the samples. The rate of propene formation increased with an increase in Ti content, reached a maximum for the sample with Ti mole fraction 0.4 and then decreased. This activity may be directly related to the surface acidity of the catalysts as surface acidity increases in the same order. The activation energies (E_a) for all the samples were calculated using Arrheneus equation in the temperature range 125–225 °C. From Table 4, it is clear that there is a broad spectrum of E_a values varying from 7.3 to 42.3 kcal/mol for mixed oxides containing different Ti mole fractions with 0.4 being the lowest value. The reason is not very clear at this stage. But, Rudham and Spiers [44] have reported E_a value 139.5 kJ/mol for isopropanol dehydration on lanthanum–Y zeolite, which is equivalent

Table 4
Rate and activation energy (E_a) for the conversion of 2-propanol to propene over sulphated ZrO_2–TiO_2 mixed oxides calcined at 600 °C[a]

Sample code	Rate of propene formation at various temperatures ($\times 10^6$,°C)				E_a (kcal/mol)	log A
	125	150	175	225		
SO_4/ZrO_2–TiO_2 (0)	30.2	35.7	–	–	14.8	16.18
SO_4/ZrO_2–TiO_2 (0.2)	163.9	623.4	–	–	18.4	15.46
SO_4/ZrO_2–TiO_2 (0.4)	161.5	937.6	–	–	7.3	12.94
SO_4/ZrO_2–TiO_2 (0.5)	59.0	638.2	–	–	8.2	13.47
SO_4/ZrO_2–TiO_2 (0.6)	15.9	229.6	–	–	9.2	13.38
SO_4/ZrO_2–TiO_2 (0.8)	–	52.26	364.9	–	42.3	28.71
SO_4/ZrO_2–TiO_2 (1.0)	–	–	35.0	829.4	5.0	23.93

Values in parentheses are the titanium mole fractions.
[a] Activation energy calculated in the temperature range 125–225 °C.

to 33.37 kcal/mol. In some cases they found E_a value as high as 149 kJ/mol (35.64 kcal/mol). In another report Parida et al. [45] have reported E_a value 7.46 and 7.83 kcal/mol for isopropanol dehydration over 8 and 10 wt.% sulphate loaded titania–silica mixed oxides, respectively. It is proposed here that the large variation in E_a values could be due to a different type of interaction between isopropanol molecule and the mixed oxide surface, or the presence of a different activation step in isopropanol dehydration process as proposed by Cunningham et al. [46] for V_2O_5 catalyst in oxygenated and non-oxygenated medium.

5. Conclusions

Highly stable ZrO_2–TiO_2 mixed oxides can be prepared by co-precipitation method. With increase in Ti content the structural stability of the samples increased and samples containing Ti mole fraction 0.4 imparts the most stable structure. Though the phase transition temperature is the same for both 50 and 60 mol% Zr containing samples, the highest specific surface area and acidity shows that the later one is more stable. The framework substitution of more electronegative Ti in ZrO_2 matrix has stabilized the surface sulphate content and it is also highest for samples containing 0.4 mole fraction of Ti. The same sample also contains highest acidity and the enhancement in surface acidity was explained by Tanabe's model. The catalytic activity of the mixed oxides for dehydration of 2-propanol shows that the sample containing Ti mol fraction 0.4 is the most active with the lowest activation energy. The rate of propene formation at 423 K shows that the rate increases with increase in Ti mole fraction until 0.4 and then decreases. This activity may be directly related to the surface acidity of the catalysts as surface acidity increases in the same order. Based on these facts one can conclude that zirconia–titania mixed oxide, with a high surface area and acidity, can be obtained by co-precipitation from a solution containing titanium mole fraction 0.4.

Acknowledgements

Financial support from Petro-Canada Ltd. for this research is acknowledged.

References

[1] K. Arata, Adv. Catal. 37 (1990) 165.
[2] A. Corma, Chem. Rev. 95 (1995) 559.
[3] M. Hino, K. Arata, J. Chem. Soc., Chem. Commun. (1980) 851.
[4] M.Y. Wen, I. Wender, J.W. Tierney, Energy Fuels 4 (1990) 372.
[5] M. Hino, K. Arata, J. Chem. Soc., Chem. Commun. (1979) 1148.
[6] S.K. Samataray, T. Mishra, K.M. parida, J. Mol. Catal. 156 (2000) 267.
[7] C. Morterra, G. Cerrato, C. Emanuel, V. Bolis, J. Catal. 142 (1993) 349.
[8] R.A. Comelli, C.R. Vera, J.M. Parera, J. Catal. 143 (1993) 616.
[9] T. Yamaguchi, T. Jin, T. Ishida, K. Tanabe, Mater. Chem. Phys. 17 (1987) 3.
[10] C.R. Vera, C.L. Pieck, K. Shimizu, C.A. Querini, J.M. Parera, J. Catal. 187 (1999) 39.
[11] Z.B. Wei, Q. Xin, X.X. Guo, E.L. Sham, P. Grange, B. Delmon, Appl. Catal. A: Gen. 63 (1990) 305.
[12] H. Tamara, M. Boulinguiez, M. Vrinat, Catal. Today 29 (1996) 209.
[13] P.D.L. Marcera, J.G. Van Oman, E.B.M. Doesburg, A. Burggraaf, J.R.H. Ross, Appl. Catal. A: Gen. 471 (1991) 363.
[14] I. Wang, W.F. Cheng, R.J. Shiau, J.C. Wu, C.S. Chung, J. Catal. 83 (1983) 428.
[15] C.-Y. Hsu, C.R. Heimbuck, C.T. Armes, B.C. Gates, J. Chem. Soc., Chem. Commun. (1992) 1645.
[16] C.H. Lin, C.Y. Hsu, J. Chem. Soc., Chem. Commun. (1992) 1479.
[17] K. Tanabe, T. Sumiyoshi, K. Shibata, T. Kiyoura, J. Kitagawa, Bull. Chem. Soc. Jpn. 47 (1974) 1064.
[18] J.A. Anderson, C. Fergusson, I.R. Ramos, A.G. Ruiz, J. Catal. 192 (2000) 344.
[19] J.B. Miller, E.I. Ko, J. Catal. 159 (1996) 58.
[20] C. Contescu, V.T. Popa, J.B. Miller, E.I. Ko, J.A. Schwarz, Chem. Eng. J. 64 (1996) 265.
[21] T. Kataoka, J.A. Dumesic, J. Catal. 112 (1988) 66.
[22] X. Song, A. Sayari, Catal. Rev. -Sci. Eng. 38 (1996) 329.
[23] R.B. Fischer in: F.J. Welcher (Ed.), Standard Methods of Chemical Analysis, Vol. 3, Part-A, 6th Edition, Van Nostrand, Princeton, NJ, 1966, p. 277.
[24] G.A. Parks, P.L. de Bruyn, J. Phys. Chem. 66 (1962) 967.
[25] J.M. Compelo, A. Garcia, J.M. Gutierrez, D. Luna, J.M. Marinas, J. Colloid Interf. Sci. 95 (1983) 388.
[26] R.A. Saleh, I.E. Wachs, S.S. Chan, C.C. Chersich, J. Catal. 98 (1989) 102.
[27] G.R. Wang, X.Q. Wang, X.S. Wang, X.S. Yu, Stud. Surf. Sci. Catal. 83 (1994) 67.
[28] F. Lonyi, J. Valyon, J. Thermal Anal. 46 (1996) 211.
[29] R. Linacero, M.L. Rojas-Cervantes, J. De, D. Lopez-Gonzalez, J. Mater. Sci. 35 (2000) 3279.
[30] F.J. Gil-Llambias, A.M. Escudy Castro, A. Lopez Agudo, J.L.D. Fierro, J. Catal. 90 (1984) 323.
[31] J.M. Dominguez, J.L. Hernandez, G. Sandoval, Appl. Catal. A: Gen. 197 (2000) 119.

[32] Y. Xia, W. Hua, Z. Gao, Appl. Catal. 185 (1999) 293.
[33] K. Nakamoto, J. Fujita, S. Tanaka, M. Kobayashi, J. Am. Chem. Soc. 28 (1957) 4904.
[34] D.A. Ward, E.I. Ko, J. Catal. 150 (1994) 18.
[35] B. Aiken, W.P. Hsu, E. Matijevic, J. Mater. Sci. 25 (1990) 1886.
[36] A. Tuel, S. Gontier, R. Teissier, J. Chem. Soc., Chem. Commun. (1996) 651.
[37] G.P. Schindler, P. Bartl, W.F. Hoelderich, Appl. Catal. A: Gen. 166 (1998) 267.
[38] G. Larsen, E. Lotero, L.M. Petkovic, D.S. Shobe, J. Catal. 169 (1997) 67.
[39] K.M. Parida, P.K. Pattanayak, J. Colloid Interf. Sci. 182 (1996) 381.
[40] F. Lonyi, J. Valyon, J. Engelhardt, F. Mizukami, J. Catal. 160 (1996) 279.
[41] A.K. Dalai, R. Sethuraman, R.O. Idem, S.P.R. Katikaneni, R.V. Malyala, N.N. Bakhshi, J. Am. Chem. Soc. Petro. Chem. Div. 44 (1999) 79.
[42] R. Srinivasan, R.A. Keogh, B.H. Davis, Appl. Catal. A: Gen. 130 (1995) 135.
[43] T. Mishra, K.M. Parida, S.B. Rao, Appl. Catal. A: Gen. 166 (1998) 115.
[44] R. Rudham, A.I. Spiers, J. Chem. Soc., Faraday Trans. 93 (7) (1997) 1445.
[45] K.M. Parida, S.K. Samantaray, H.K. Mishra, J. Colloid Interf. Sci. 216 (1999) 127.
[46] J. Cunningham, M. Ilyas, J. Nunan, Can. J. Chem. 62 (1984) 785.